New Mechanistic Insights from Structural Studies of the Oxygen-Sensing Domain of *Bradyrhizobium japonicum* FixL[†,‡]

Weimin Gong,[§] Bing Hao,[§] and Michael K. Chan*

Departments of Biochemistry and Chemistry, The Ohio State University, 484 West 12th Avenue, Columbus, Ohio 43210

ABSTRACT: The FixL heme domain serves as the dioxygen switch in the FixL/FixJ two-component system of *Rhizobia*. Recent structural studies of the *Bradyrhizobium japonicum* FixL heme domain (BjFixLH) have suggested an allosteric mechanism that is distinct from the classical hemoglobin model. To gain further insight into the FixL sensing mechanism, structures of BjFixLH bound to dioxygen, imidazole, and nitric oxide have been determined. These structures, particularly the structure of BjFixLH bound to its physiological ligand, dioxygen, have helped to address a number of important issues relevant to the BjFixLH sensing mechanism. On the basis of the oxy-BjFixLH structure, a conserved arginine is found to stabilize the dioxygen ligand in a mode reminiscent of the distal histidine in classical myoglobins and hemoglobins. The structure of BjFixLH bound to imidazole elucidates the structural requirements for accommodating sterically bulky ligands. Finally, the structure of BjFixLH bound to nitric oxide provides evidence for a structural intermediate in the heme-driven conformational change.

FixL proteins are biological oxygen sensors that regulate nitrogen fixation gene expression in *Rhizobia* (*1–3*). FixL proteins are comprised of two distinct domains. Near the N-terminus is a heme-based oxygen-sensing domain that belongs to the PAS superfamily (*4*). At the C-terminus is a histidine kinase domain, which in its active state undergoes autophosphorylation and then transfers the phosphoryl group to FixJ, its associated response regulator. Phosphorylated FixJ binds to the nifK promoter initiating nitrogen fixation gene expression (*5*).

A spin-state mechanism has been proposed for FixL (*6*). While the functional form of the FixL heme is thought to be ferrous, the kinase activity has been shown to be correlated with the spin state of the metal. When the heme iron is high spin, as in unliganded ferrous or ferric FixL, the kinase is active. Binding of strong-field ligands (oxygen, cyanide, carbon monoxide) inactivates the kinase activity.

We recently reported the crystal structures of the *Bradyrhizobium japonicum* FixL heme domain (BjFixLH)[1] in its unliganded ferric (met-BjFixLH) and cyanide-bound (cyanomet-BjFixLH) forms (*7*). Comparison of these structures revealed a conformational change in a region between the F$_\alpha$-helix and the G$_\beta$-strand, termed the FG loop. As in the classical allosteric protein, hemoglobin, the conformational change is probably driven by changes in the structure of the heme active site upon ligand binding (*8*). Unlike hemoglobin, however, the proximal histidine remains in approximately the same location in both met- and cyanomet-BjFixLH. Instead, ligand binding induces a change in the nonplanar distortion of the heme that is transmitted to the polypeptide via salt-bridge and hydrogen-bonding interactions between the propionate side chains of the heme and the protein residues of the FG loop. Hence, FixL proteins represent a distinct class of heme proteins, in terms of both their function and their signaling mechanism (*3, 9–11*).

The structural determination of other ligand-bound forms of BjFixLH is important both to elucidate the details of ligand binding and to further refine our understanding of the allosteric mechanism of BjFixLH. Since dioxygen is the physiological ligand of BjFixL, the structure of its oxygen-bound form (oxy-BjFixLH) is important to determine whether dioxygen binding triggers the same protein conformational change as cyanide. This would help to assess the functional relevance of the previous observations. Another important structure is the structure of imidazole-bound BjFixLH (imidazole-BjFixLH). This structure would help to elucidate how the heme pocket adjusts to accommodate relatively bulky ligands—a question of particular relevance since the met- and cyanomet-BjFixLH structures indicate a sterically crowded pocket. A final target of interest is the structure of BjFixLH bound to nitric oxide (NO-BjFixLH). It has been suggested that BjFixL serves as an NO sensor. The structure of NO-BjFixLH would help to determine whether nitric oxide induces the same conformational change as dioxygen. To address these issues, we have determined the structures of oxy-BjFixLH, imidazole-BjFixLH, and NO-BjFixLH and here report our results.

1 Abbreviations: BjFixLH, *Bradyrhizobium japonicum* FixL heme domain; met-BjFixLH, unliganded ferric BjFixLH; cyanomet-BjFixLH, cyanide-bound met-BjFixLH; oxy-BjFixLH, dioxygen-bound BjFixLH; imidazole-BjFixLH, imidazole-bound BjFixLH; NO-BjFixLH, nitric oxide-bound BjFixLH.

Table 1: Data Processing and Refinement Statistics

crystal	oxy	imidazole	NO
space group	*R*32	*R*32	*R*32
cell parameters (Å)	*a* = 127.37,	*a* = 125.97,	*a* = 127.15,
	c = 58.58	*c* = 58.73	*c* = 58.25
resolution range (Å)	20.0−2.3	20.0−2.6	20.0−2.5
no. of reflections	57805	53578	45555
no. of unique reflections	7990	5137	6138
residues	154−269	154−269	153−270
no. of protein (ligand) atoms	957 (2)	957 (5)	975 (2)
no. of solvent	98	55	81
temp factor of protein (Å^2)	25.0	30.3	23.0
temp factor of ligand (Å^2)	21.5	26.8	19.5
completeness (%)^a	97.6 (94.9)	91.9 (83.3)	97.0 (92.3)
R_{merge} (%)^{a,b}	4.8 (25.6)	5.8 (26.0)	5.9 (29.3)
R factor (%)^c	20.6	19.5	20.5
R_{free} (%)^d	25.0	26.3	25.2
rmsd of bond distance (Å)	0.016	0.014	0.014
rmsd of bond angles (deg)	1.80	1.82	1.78

^{a} The numbers in parentheses are for the highest resolution shell.
^{b} $R_{merge}(I) = \sum_h\sum_i|I_i - I|/\sum_h\sum_iI$, where I is the mean intensity of the i observations of reflection h. ^{c} *R* factor = $100(\sum|F_o - F_c|/\sum|F_o|)$, where F_o and F_c are the observed and calculated structure factors, respectively. ^{d} R_{free} was calculated using 8% of the reflections.

MATERIALS AND METHODS

Crystallization and Data Collection. Met-BjFixLH crystals were prepared as reported previously (*7*). Oxy-BjFixLH crystals were generated by soaking met-BjFixLH crystals with solutions of synthetic mother liquor containing 100 mM ascorbic acid and increasing concentrations of glycerol [up to 40% (v/v)]. Imidazole-BjFixLH crystals were prepared by soaking met-BjFixLH crystals with solutions of synthetic mother liquor containing 20 mM imidazole. The NO-BjFixLH crystals were obtained by soaking met-BjFixLH crystals with glycerol followed by addition of diethylamine NONOate (Cayman Chemical Co.). The NO-BjFixLH crystals were sealed under positive NO pressure for 1 day. Prior to data collection, each crystal was mounted on a cryoloop and cooled in a stream of nitrogen at 100 K.

The diffraction data were collected at 100 K on a CCD detector on Beamline X4A at the National Synchrotron Light Source in Brookhaven National Laboratory. The wavelength for all the data sets was 1.2830 Å. Data processing and reduction were performed using DENZO and SCALEPACK (Table 1) (*12*).

Structure Determination and Refinement. Each of the ligand-bound structures of BjFixLH was determined using the met-BjFixLH structure (PDB entry 1DRM) as the starting model. The residues comprising the FG loop (from residue Thr 209 to His 219) and the solvent molecules were omitted in the initial refinement of each structure. Model building and refinement were performed using the programs O (*13*) and X-PLOR 3.851 (*14*), respectively. A flat bulk solvent correction and an overall anisotropic *B*-factor scaling were applied to the diffraction data. The ligands, solvent molecules, and residues forming the FG loop were modeled on the basis of the resulting $2F_o - F_c$ and $F_o - F_c$ electron density maps. The quality of the model for each structure was evaluated using PROCHECK (*15*). All stereochemical parameters in each structure were within the acceptable ranges. Figures were prepared using the programs Molscript (*16*), Raster 3D (*17*), and XtalView (*18*). We note here that, due to a typographical error, a salt bridge between Glu 182

and Arg 226 was incorrectly reported (*7*). The correct interaction is between Glu 182 and Arg 227.

RESULTS AND DISCUSSION

The general protein fold of each ligand-bound form of BjFixLH is similar to those of the met- and cyanomet-BjFixLH structures determined previously (*7*). The oxy-BjFixLH structure is shown in Figure 1A. Alignment of each of the different structures by least-squares refinement reveals that the C$_\alpha$ positions for all BjFixLH structures lie within 0.2 Å for all residues, except for those within the critical FG loop (Thr 209 to His 220). For the residues within this FG loop, the average differences in the C$_\alpha$ positions are significantly larger (up to 2.0 Å). In each of the ligand-bound structures, oxy-BjFixLH, imidazole-BjFixL, and NO-BjFixL, the temperature factors for the ligands are comparable to that of the protein (Table 1).

Nature of the Distal Ligand in Oxy-BjFixLH. Since the ferric heme of met-BjFixLH does not bind dioxygen (*1*), oxy-BjFixLH crystals were obtained by treating met-BjFixLH crystals with ascorbic acid (to reduce the heme iron) in the presence of dioxygen. The $2F_o - F_c$ and $F_o - F_c$ electron density maps revealed density in the heme pocket, consistent with a dioxygen ligand that binds the heme iron in a bent mode (∠Fe−O−O ~124°) (Figures 1C and 2B). The plane formed by the heme iron and the bent dioxygen ligand appears to be aligned with the plane of the proximal histidine ring.

The binding of dioxygen results in a shift of the FG loop similar to that observed in cyanomet-BjFixLH (*7*). In both forms, the binding of the strong-field ligand alters the nonplanarity of the heme, resulting in a shift in the positions of the two heme propionate side chains. This change in the heme nonplanarity is most dramatic near heme propionate 7. The binding of oxygen to the heme causes the first carbon of heme propionate 7 (CAA) and the pyrrole carbon to which heme propionate 7 is attached (C2A) to shift by 1.10 and 0.83 Å, respectively. As the expected error in the atomic positions in these structures is approximately 0.3 Å at the current resolution, it seems fairly certain that changes in the heme nonplanarity do play a role in the heme-driven conformational change of BjFixL.

The movement of the propionate side chains, in turn, is transmitted to the polypeptide via salt bridges to His 214, whose translation stabilizes the FG loop in an alternative conformation that lies farther from the heme. As a result of these shifts, both oxy-BjFixLH and cyanomet-BjFixLH exhibit similar allosteric changes, with Arg 220 losing its salt bridge to heme propionate 7, while Arg 206 moves to form a salt bridge to heme propionate 6. The magnitude of the shift in oxy-BjFixLH, however, appears to be larger than in cyanomet-BjFixLH (Table 2). While this could indicate a true structural difference, it may also reflect the proportion of the ligand-bound and unbound molecules in the two crystal structures.

One of the fundamental issues regarding FixL proteins has been whether they utilize a hydrogen bond donor to stabilize the binding of dioxygen to the heme. Historical precedent for hydrogen-bonding interactions in an oxygen-binding heme protein has been demonstrated in classical myoglobins
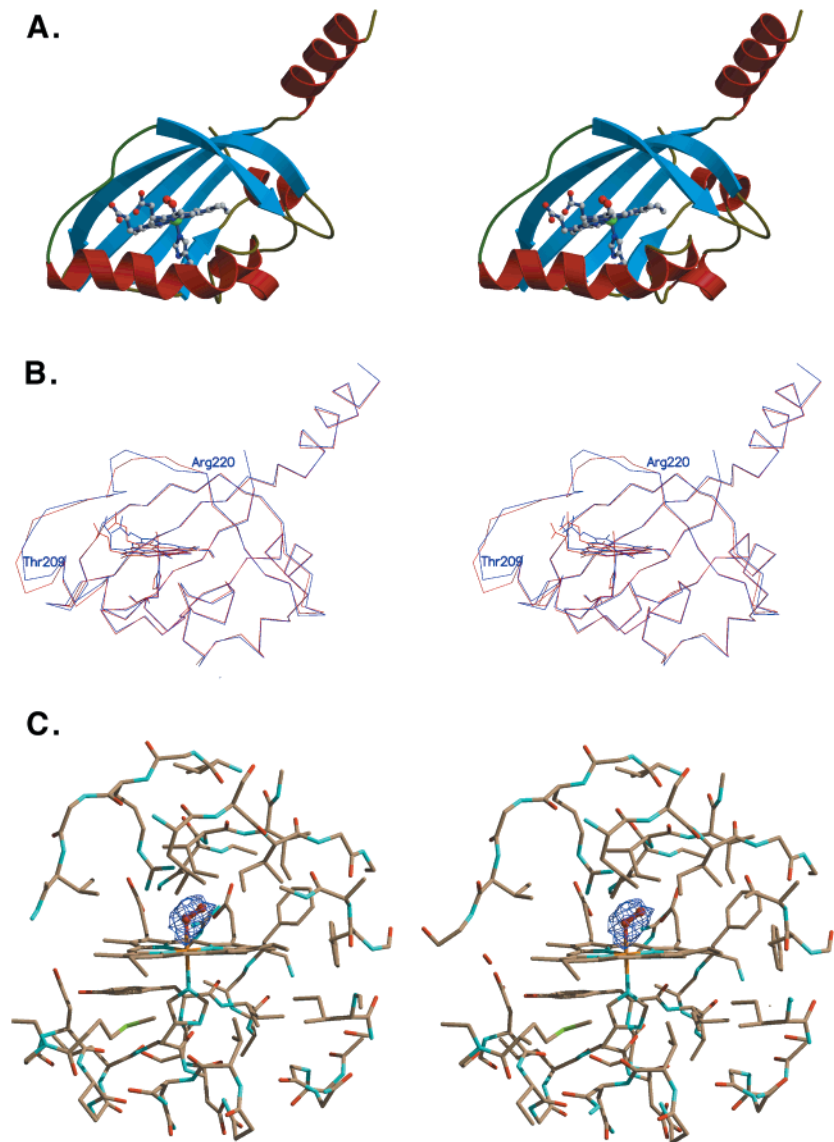
FIGURE 1: (A) Ribbon diagram of oxy-BjFixLH colored by secondary structure (α-helix, red; β-strand, blue; random coil, yellow; FG loop, green). The atoms of the heme, dioxygen ligand, and proximal histidine are depicted as ball-and-stick models and are colored by element (carbon, gray; oxygen, red; nitrogen, blue; iron, green). (B) Comparison of the C_α positions, the proximal histidine, and the heme for met-BjFixLH (blue) and oxy-BjFixLH (red). The two molecules were aligned by a least-squares fit over the entire protein. (C) $F_o - F_c$ difference map (4.0σ) of the oxy-BjFixL heme pocket with the dioxygen ligand omitted.

Table 2: Average Positional Differences (Å) in the C_α Atoms of the FG Loop (Thr 209 to His 219) for Different Forms of BjFixLH

ligand-bound forms	met	NO	cyanomet	imidazole	oxy
met					
NO	0.1				
cyanomet	0.9	0.8			
imidazole	1.4	1.4	0.7		
oxy	1.7	1.6	0.9	0.4	

and hemoglobins that utilize a distal histidine (residue E7) to anchor the dioxygen ligand. Even in *Aplysia* (*19*) and elephant myoglobins (*20*) that both lack the E7 histidine, a stabilizing interaction is provided by an E10 arginine or B10 phenylalanine, respectively. Surprisingly, in our previous cyanomet-BjFixLH structure, however, no hydrogen-bonding residue was found in close proximity to the cyanide ligand, the distal pocket being formed solely by hydrophobic residues: Ile 215, Ile 216, Val 222, Met 234, Leu 236, and Ile 238 (*7*).

The observations from the cyanomet-BjFixLH structure were unusual in light of the similarity of the dioxygen dissociation rates for FixL proteins and myoglobins that have been used to argue strongly for the existence of a distal ligand (*3, 21*). In addition, the binding of water to the ferric heme in myoglobin and the absence of such a bound water in ferric FixL have been used to suggest that the putative distal ligand is a hydrogen bond donor, but not a hydrogen bond acceptor. These arguments ruled out a distal histidine but suggested that the guanidinium side chain of an arginine or the positive edge of a phenylalanine could serve as the putative hydrogen bond donor (*21*).

The existence and identity of the distal ligand are provided by the oxy-BjFixLH structure. While in cyanomet-BjFixLH and met-BjFixLH Arg 220 remains in essentially the same position, in oxy-BjFixLH the guanidinium side chain of Arg 220 rotates into the heme pocket and forms a hydrogen bond with the bound dioxygen ligand. This change is fairly
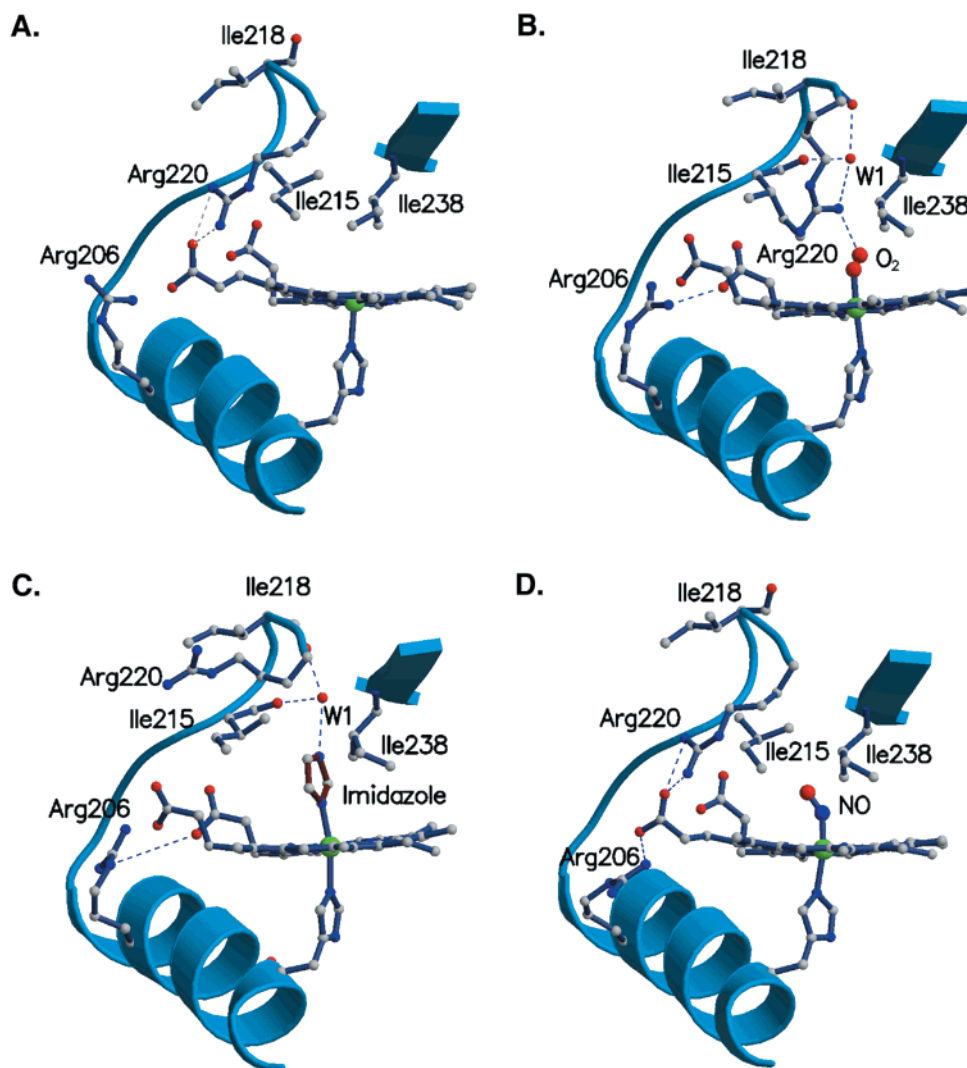
FIGURE 2: Ribbon and ball-and-stick model diagrams of the BjFixLH heme binding pocket for (A) met-BjFixLH, (B) oxy-BjFixLH, (C) imidazole-BjFixLH, and (D) NO-BjFixLH.

dramatic, requiring a rotation of ∼170° around the $C_\alpha-C_\beta$ bond of Arg 220 (Figure 2B).

The oxy-BjFixLH structure also reveals another important aspect of the conformational change. Concomitant with the shift of the FG loop is a reorientation of the main-chain atoms of Ile 218. While in met-BjFixLH the carbonyl of Ile 218 points toward the solvent, in oxy-BjFixLH, as a result of the conformational change, the carbonyl of Ile 218 rotates into the heme pocket forming a hydrogen-bonding interaction with a water molecule (Figure 2B). This water, in turn, forms a hydrogen bond with Arg 220 that may help to stabilize the position of Arg 220 for optimal interaction with the dioxygen ligand.

Conserved Mode of Dioxygen Binding in Heme Proteins. The oxy-BjFixLH structure is also important for comparisons to other heme proteins that bind dioxygen. Analysis of the dioxygen binding modes in these proteins could provide insight into the factors that contribute to the binding affinity of dioxygen ligands. While such analyses have been performed previously (22, 23), these studies have been limited by the general paucity of structures of dioxygen-bound heme proteins and model compounds.

Superposition of the heme cofactors in oxy-BjFixLH and in the 1.0 Å structure of sperm whale oxymyoglobin (PDB

entry 1A6M) reveals similar orientations of the heme, proximal histidine, and distal ligand relative to the bound dioxygen ligand (Figure 3). The aromatic ring of the proximal histidine and the plane of the bent (Fe−O−O) dioxygen ligand appear aligned, while the hydrogen bond from the distal ligand appears to originate from a similar orientation. The conservation of these features in distinctly different heme proteins supports notions that the orientation of the dioxygen ligand, proximal histidine, and distal ligand contributes to the dioxygen binding affinity (22).

Steric Rearrangements Required for Binding of Imidazole to BjFixLH. Imidazole can be utilized to study the influence of steric factors on ligand binding. Studies of native and mutant myoglobins have shown that the imidazole association rates are largely governed by steric factors (24). Indeed, the relatively large imidazole association rates of BjFixL and BjFixLH have been used to suggest an unhindered distal cavity (24). Strangely, these results differ somewhat from the observations based on the met-BjFixLH structure that reveal several hydrophobic residues in close proximity to the distal binding site. To elucidate the required shifts necessary to accommodate bulky ligands such as imidazole, the structure of BjFixLH bound to imidazole was determined.
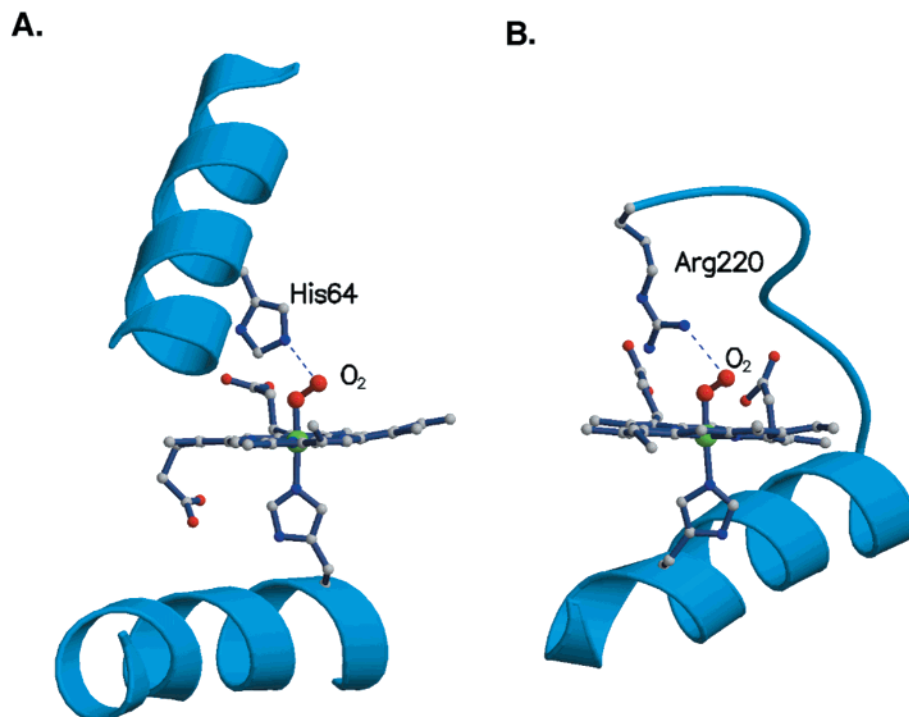
FIGURE 3: Structural comparison of the heme environment for (A) sperm whale oxymyoglobin and (B) oxy-BjFixLH.

The structure of the imidazole-BjFixLH heme pocket is depicted in Figure 2C. The $2F_o - F_c$ and $F_o - F_c$ electron density maps clearly reveal density consistent with a bound imidazole ligand. As observed for the dioxygen ligand in oxy-BjFixLH, the plane of the imidazole ring appears to be aligned with the plane of the proximal histidine.

The binding of imidazole to the FixL heme has been shown to turn off the kinase activity (M. A. Gilles-Gonzalez, unpublished results). Consistent with this observation, the structure of imidazole-BjFixLH reveals changes in the FG loop that are similar to those observed in oxy- and cyanomet-BjFixLH. Comparison of these structures reveals that the shift of the FG loop in imidazole-BjFixLH is nearly the same as in oxy-BjFixLH (Table 2). As in oxy-BjFixLH, a water molecule located within the distal pocket interacts with the carbonyl of Ile 218. Unlike oxy-BjFixLH, however, in imidazole-BjFixLH the water in the distal pocket hydrogen-bonds the imidazole ligand directly, while the guanidinium side chain of Arg 220 adopts a position outside of the heme pocket (Figure 2C).

As mentioned previously, the binding of imidazole to the heme requires a reorientation of the distal residues in order to accommodate the larger ligand. The nature of these adjustments is revealed by the imidazole-BjFixLH structure. While some room is provided by a change in the rotamer of Ile 238, the majority of the space appears to be provided by a 2.2 Å translation of Ile 215 that is associated with a shift of the FG loop away from the heme pocket. Favorable hydrogen-bonding interactions between the imidazole ligand and the water that lies within the heme pocket may also contribute to the binding of imidazole to BjFixLH.

Probing the Ability of BjFixLH To Sense Nitric Oxide. While dioxygen is clearly the physiological ligand of FixL proteins, it has also been speculated that nitric oxide could serve as a secondary ligand (24). In support of this hypothesis, nitric oxide has been noted to be the potential product of denitrification by *Rhizobia* (25), while sensing of nitric oxide by heme proteins has been demonstrated for the soluble guanylyl cyclase of vertebrates (26). In addition, spectroscopic studies of the *Rhizobium meliloti* FixL (Rm-FixL) have been used to suggest that NO-RmFixL serves as a good model for oxy-RmFixL (27). If nitric oxide is indeed a physiological ligand of FixL, however, it should be able to induce the same conformational changes as dioxygen. To test this concept, the structure of BjFixLH bound to nitric oxide was determined.

The NO-BjFixLH structure is depicted in Figure 2D. The $2F_o - F_c$ and $F_o - F_c$ electron density maps reveal density in the distal pocket consistent with the presence of a bent nitrosyl ligand bound to the heme iron ($\angle$Fe$-$N$-$O $\sim$146°). Importantly, however, unlike oxy- and imidazole-BjFixLH, no major conformational change of the FG loop is observed. Comparison of the C_α atoms within the critical FG loops of met-BjFixLH and NO-BjFixLH yields an average positional difference of only 0.1 Å (Table 2). The arms of the two heme propionates remain in approximately the same positions as well, suggesting that nitric oxide is not a secondary ligand of BjFixL.

An important consideration, however, is the oxidation state of the heme. As the physiologically relevant state of BjFixLH heme is ferrous, and the crystals of NO-BjFixLH were prepared from met-BjFixLH crystals, it could be argued that the NO-BjFixLH structure does not represent the physiologically relevant state. Analysis of the NO-BjFixLH structure and comparison with isolated nitrosyl iron porphyrin model complexes, however, suggest that the iron in the NO-BjFixLH structure is ferrous. Studies of nitrosyl iron porphyrins reveal that the Fe$-$N$-$O angle is linear in nitrosyl iron(III) porphyrins and bent in nitrosyl iron(II) porphyrins (consistent with the NO-BjFixLH structure) (28$-$31). Indeed, in agreement with these observations, resonance Raman
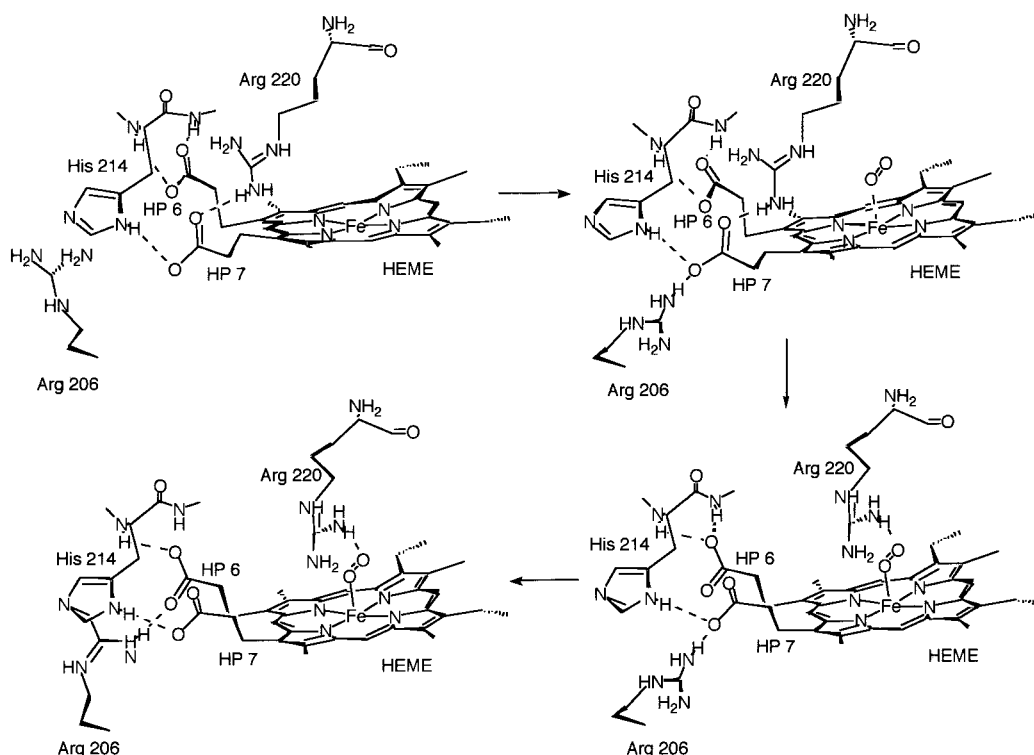
FIGURE 4: Proposed mechanism for the heme-driven conformational change of BjFixL. The heme propionate 6 and heme propionate 7 side chains are labeled HP6 and HP7, respectively.

studies of ferrous NO-RmFixL suggest a bent Fe−NO ligand (*27*).

The reduction of ferric porphyrins by nitric oxide is precedented. Indeed, attempts to prepare nitrosyl iron(III) porphyrins have been hindered by the propensity for photoreduction of the heme—particularly in the presence of suitable NO^+ acceptors such as water (*31*). Similarly, crystals of the ferriheme-NO nitrophorin yielded the structure of the ferroheme-NO nitrophorin due to photoreduction in the X-ray beam (*32*). Presumably, photoreduction of the ferric heme has occurred in our NO-BjFixLH crystals as well.

On the basis of the FixL spin-state mechanism (*6*), the absence of a shift in the FG loop suggests that the ligand field strength of the bent nitrosyl ligand is not large enough to induce the required spin-state change. While this is unusual, it is possible that the protein tension contributes to the barrier for the spin-state change. An alternative explanation is possible, however, based on structures of nitrosyl iron-(II) porphyrins. While the iron-porphinato nitrogen bonds in nitrosyl iron(II) porphyrins are comparable to those of other low-spin iron(II) complexes, the displacement of the iron atom out of the porphyrin plane and the Fe−N_b bond of the axial ligand *trans* to the NO ligand differ significantly in these complexes (*29*). The Fe−N_b bonds in nitrosyl iron(II) porphyrins are longer by up to 0.3 Å and exhibit larger out-of-plane metal displacements (*29*). Hence, an alternative explanation is that the heme iron in NO-BjFixLH is low spin but that the conformational change does not take place due to inherent ruffling of NO-bound hemes.

Whatever the origin, the absence of a protein conformational change in the NO-BjFixLH structure argues against a role for BjFixL in nitric oxide sensing. It is important to point out, however, that the interaction of the heme domain with the kinase domain could lead to differences in the ligand binding properties of BjFixLH and BjFixL (*11*). Hence, a measurement of the kinase activity of BjFixL in the presence of NO would be important to resolve this issue conclusively.

Support for a Structural Intermediate in the Heme-Driven Conformational Change. A detailed examination of the NO-BjFixLH structure reveals that although there is no shift of the FG loop, the binding of nitric oxide to the heme still appears to influence the heme distortion. The heme nonplanarity in NO-BjFixLH appears to be halfway between that of met-BjFixLH and oxy-BjFixLH. Addition of NO results in a shift of 0.44 Å for the first carbon of heme propionate 7 (CAA) and a shift of 0.28 Å for the pyrrole carbon to which heme propionate 7 is attached (C2A). These results suggest that while ligand binding contributes to the flattening of the heme, a further distortion is required to trigger the protein conformational change.

The significance of these observations is that it supports the existence of two distinct protein conformations in BjFixL. Such properties are consistent with the two-state model characteristic of most allosteric proteins, hemoglobin being the classical paradigm (*33*). Hence, while it is the change in the heme ruffling that drives the conformational change, there is tension that must be overcome for the FG loop to alter its conformation. A possible candidate for this tension may be the salt bridge between heme propionate 7 and Arg 220, a residue that is conserved in all three proteins that contain the FixL heme domain (*34*). Presumably, once the shift in the FG loop takes place, it alters its interactions with the kinase domain. Hence, we hypothesize that it is not the absolute magnitude of the conformation change in the heme domain that is critical, only that it be enough to switch its interactions with the kinase domain.

Further comparison of the NO-BjFixLH structure with the other BjFixLH structures reveals another subtlety that may

be significant. In the unliganded met-BjFixLH structure, the guanidinium side chain of Arg 206 interacts with the main-chain carbonyl and side-chain carboxylate of Asp 212. In the cyanomet-, imidazole-, and oxy-BjFixLH structures, all of which exhibit the typical conformational change, Arg 206 appears to shift slightly to a position that interacts with the carbonyl of Asp 212 and the carboxylate of heme propionate 6. In NO-BjFixLH, however, the position of Arg 206 differs from either of these structures, and instead the side chain of Arg 206 is found to form a salt bridge with heme propionate 7. No other change in the polypeptide is apparent.

These observations lead us to suggest that the NO-BjFixLH structure may model an intermediate in the heme-driven conformational change. On the basis of this hypothesis, we have developed an allosteric mechanism for BjFixLH that involves discrete intermediates (Figure 4). In this mechanism, the binding of ligands (whether strong field or weak field) induces a change in the ruffling of the porphyrin to the extent that Arg 206 rotates from its initial position observed in met-BjFixLH to a position where it forms a salt bridge with heme propionate 7. The importance of this interaction is that the positive charge of Arg 206 could then be used to weaken the salt bridge formed between heme propionate 7 and Arg 220. Loss of the heme propionate 7−Arg 220 salt bridge is required for the conformational change to take place.

Such a role for Arg 206 would be congruent with the fact that this residue is conserved as positively charged amino acid (arginine or histidine) in all FixL heme domains characterized to date (*34*). Once the salt bridge has been broken, presumably as describe above, a spin-state change of the heme iron induces a further flattening of the porphyrin ring that helps to promote the FG loop shift. In a subsequent step, Arg 206 could then move to interact with its final partner, heme propionate 6, completing the observed conformational change.

CONCLUSIONS

This study addresses several fundamental issues relevant to the mechanisms of oxygen binding and sensing by heme proteins. The structure of oxy-BjFixLH provides further evidence supporting the importance of distal hydrogen-bonding interactions in stabilizing dioxygen binding to heme centers. The conservation of the orientation of the proximal histidine, heme, dioxygen ligand, and distal residue in both BjFixLH and myoglobins suggests that there are definite features that promote optimal dioxygen binding affinity.

The structures of the other ligand-bound forms also yield new insights. The imidazole-BjFixLH structure reveals how the protein adjusts to accommodate larger ligands. Perhaps more intriguing, however, is the structure of NO-BjFixLH that appears to both provide evidence against a role for FixL proteins in nitric oxide sensing and suggest the existence of a potential intermediate in the BjFixLH conformational change. Given the difference of FixL's allosteric mechanism with that of hemoglobin, the discovery and characterization this intermediate provide important information regarding the mechanisms of sensing by heme cofactors. While the specific details are likely to differ, the global features of this mechanism could have relevance to the growing family of sensory heme proteins.

REFERENCES

1. Gilles-Gonzalez, M. A., Ditta, G., and Helinski, D. R. (1991) *Nature 350*, 170−172.
2. Gilles-Gonzalez, M. A., and Gonzalez, G. (1993) *J. Biol. Chem. 268*, 16293−16297.
3. Gilles-Gonzalez, M. A., Gonzalez, G., Perutz, M. F., Kiger, L., Marden, M., and Poyart, C. (1994) *Biochemistry 33*, 8067−8073.
4. Zhulin, I. B., Taylor, B. L., and Dixon, R. (1997) *Trends Biochem. Sci. 22*, 331−333.
5. Agron, P. G., Ditta, G. S., and Helinski, D. R. (1993) *Proc. Natl. Acad. Sci. U.S.A. 90*, 3506−3510.
6. Gilles-Gonzalez, M. A., Gonzalez, G., and Perutz, M. F. (1995) *Biochemistry 34*, 232−236.
7. Gong, W., Hao, B., Mansy, S. S., Gonzalez, G., Gilles-Gonzalez, M. A., and Chan, M. K. (1998) *Proc. Natl. Acad. Sci. U.S.A. 95*, 15177−15182.
8. Perutz, M. F. (1970) *Nature 228*, 726−739.
9. Pellequer, J. L., Brudler, R., and Getzoff, E. D. (1999) *Curr. Biol. 9*, R416−R418.
10. Rodgers, K. (1999) *Curr. Opin. Chem. Biol. 3*, 158−167.
11. Perutz, M. F., Paoli, M., and Lesk, A. M. (1999) *Chem. Biol. 6*, R291−R297.
12. Otwinowski, Z., and Minor, W. (1997) *Methods Enzymol. 276*, 307−326.
13. Jones, T. A., Zou, J. Y., Cowan, S. W., and Kjeldgaard, M. (1991) *Acta Crystallogr. A47*, 110−119.
14. Brunger, A. T. (1993) *X-PLOR Version 3.1 Manual*, Yale University, New Haven, CT.
15. Laskowski, R. A., MacArthur, M. W., Moss, D. S., and Thornton, J. M. (1993) *J. Appl. Crystallogr. 26*, 283−291.
16. Kraulis, P. (1991) *J. Appl. Crystallogr. 24*, 946−950.
17. Merritt, E., and Murphy, M. (1994) *Acta Crystallogr. D50*, 869−873.
18. McRee, D. E. (1993) *Practical Protein Crystallography*, Academic Press, Inc., San Diego, CA.
19. Conti, E., Moser, C., Rizzi, M., Mattevi, A., Lionetti, C., Coda, A., Ascenzi, P., Brunori, M., and Bolognesi, M. (1993) *J. Mol. Biol. 233*, 498−508.
20. Bisig, D. A., Di Iorio, E. E., Diederichs, K., Winterhalter, K. H., and Piontek, K. (1995) *J. Biol. Chem. 270*, 20754−20762.
21. Mansy, S. S., Olson, J. S., Gonzalez, G., and Gilles-Gonzalez, M. A. (1998) *Biochemistry 37*, 12452−12457.
22. Lavalette, D., Tetreau, G., Mispelter, J., Momenteau, M., and Lhoste, J. M. (1984) *Eur. J. Biochem. 145*, 555−565.
23. Momenteau, M., and Reed, C. A. (1994) *Chem. Rev. 94*, 659−698.
24. Winkler, W. C., Gonzalez, G., Wittenberg, J. B., Hille, R., Dakappagari, N., Jacob, A., Gonzalez, L. A., and Gilles-Gonzalez, M. A. (1996) *Chem. Biol. 3*, 841−850.
25. Chan, Y. K., and Wheatcroft, R. (1992) *J. Bacteriol. 175*, 19−26.
26. Zhao, Y., Hoganson, C., Babcock, G. T., and Marletta, M. A. (1998) *Biochemistry 37*, 12458−12464.
27. Lukat-Rodgers, G. S., and Rodgers, K. R. (1997) *Biochemistry 36*, 4178−4187.
28. Scheidt, W. R., and Piciulo, P. L. (1976) *J. Am. Chem. Soc. 98*, 1913−1919.
29. Scheidt, W. R., Brinegar, A. C., Ferro, E. B., and Kirner, J. F. (1977) *J. Am. Chem. Soc. 99*, 7315−7322.

30. Ellison, M. K., and Scheidt, W. R. (1997) *J. Am. Chem. Soc. 119*, 7404−7405.

31. Ellison, M. K., and Scheidt, W. R. (1999) *J. Am. Chem. Soc. 121*, 5210−5219.

32. Ding, X. D., Weichsel, A., Andersen, J. F., Shokhireva, T. K., Balfour, C., Pierik, A. J., Averill, B. A., Montfort, W. R., and Walker, F. A. (1999) *J. Am. Chem. Soc. 121*, 128−138.

33. Perutz, M. F. (1989) *Mechanisms of cooperativity and allosteric regulation in proteins*, Cambridge University Press, Cambridge.

34. Taylor, B. L., and Zhulin, L. B. (1999) *Microbiol. Mol. Biol. Rev. 63*, 479−506.